AD_____

Award Number: W81XWH-16-1-0289

TITLE: Cotargeting the lncRNA-PIP3 Interaction and AKT/PI3K Signaling Axis: A Novel Paradigm for Treating Triple-Negative Breast Cancer

PRINCIPAL INVESTIGATOR: Dr. Liuqing Yang

CONTRACTING ORGANIZATION: University of Texas MD Anderson Cancer Center
Houston, TX 77030

REPORT DATE: October 2018

TYPE OF REPORT: Annual

PREPARED FOR: U.S. Army Medical Research and Materiel Command
Fort Detrick, Maryland 21702-5012

# REPORT DOCUMENTATION PAGE

*Form Approved*
*OMB No. 0704-0188*



| 1. REPORT DATE | 2. REPORT TYPE | 3. DATES COVERED |
|---|---|---|
| October 2018 | Annual | 15 Sep 2017 - 14 Sep 2018 |

**4. TITLE AND SUBTITLE**

Cotargeting the lncRNA-PIP3 Interaction and AKT/PI3K Signaling Axis: A Novel Paradigm for Treating Triple-Negative Breast Cancer

**5a. CONTRACT NUMBER**

**5b. GRANT NUMBER**
W81XWH-16-1-0289

**5c. PROGRAM ELEMENT NUMBER**

**6. AUTHOR(S)**

Liuqing Yang

E-Mail: lyang7@mdanderson.org

**5d. PROJECT NUMBER**

**5e. TASK NUMBER**

**5f. WORK UNIT NUMBER**

**7. PERFORMING ORGANIZATION NAME(S) AND ADDRESS(ES)**

UNIVERSITY OF TEXAS M D
ANDERSON CANCER
HOUSTON TX 77030-0417

**8. PERFORMING ORGANIZATION REPORT NUMBER**

**9. SPONSORING / MONITORING AGENCY NAME(S) AND ADDRESS(ES)**

U.S. Army Medical Research and Materiel Command
Fort Detrick, Maryland 21702-5012

**10. SPONSOR/MONITOR'S ACRONYM(S)**

**11. SPONSOR/MONITOR'S REPORT NUMBER(S)**

**12. DISTRIBUTION / AVAILABILITY STATEMENT**

Approved for Public Release; Distribution Unlimited

**13. SUPPLEMENTARY NOTES**

**14. ABSTRACT**

Triple-negative breast cancers (TNBC) does not respond to endocrine therapies or HER2-targeted therapies are difficult to attack. Hyperactive AKT/PI3K signaling is a common feature of TNBC and its inhibition has potent antitumor consequences. Unfortunately, targeted cancer therapy results in short-lived benefits that are followed by acquired resistance that arises through unknown mechanisms. Long noncoding RNAs (lncRNAs) are aberrantly expressed in a broad spectrum of cancers, including breast cancer, and play key roles in promoting and maintaining cancer cell characteristics, which makes these molecules attractive therapeutic targets. We identified the expression of a lncRNA, LINK-A is upregulated in TNBC tissues compared to non-TNBC breast cancer tissues. LINK-A associated with cellular lipid components which promotes EGF-induced AKT activation. The proposed study will identify the mechanism by which lncRNAs regulate the AKT/PI3K pathway in order to devise a co-targeting strategy. To address our hypothesis that LINK-A functions to regulate PI3K-AKT signaling pathway via its interaction with PIP3 in TNBC cells and that this mechanism may impact the efficacy of PI3K-AKT inhibition, we will identify the mechanism by which specific LINK-A-PIP3 interactions influence AKT activation; examine the functional role of LINK-A in regulating PI3K-AKT pathway in TNBC; and evaluate the effects of combined inhibition of LINK-A with pharmacologic inhibitors of PI3K-AKT pathway on TNBC progression. The results from the proposed study will bring innovative and cogent lncRNA-based tactics to attack central problems in breast cancer research and offer a notable advance in the fight against TNBC by highlighting lncRNAs as a class of drug targets for breast cancer metastasis.

**15. SUBJECT TERMS**

TNBC, Long non-coding RNA, PIP3, AKT, Phosphorylation, Locked Nucleic Acids, LNA, AKT inhibitor, Tumorigenesis

| 16. SECURITY CLASSIFICATION OF: | | | 17. LIMITATION OF ABSTRACT | 18. NUMBER OF PAGES | 19a. NAME OF RESPONSIBLE PERSON |
|---|---|---|---|---|---|
| a. REPORT | b. ABSTRACT | c. THIS PAGE | | | USAMRMC |
| Unclassified | Unclassified | Unclassified | Unclassified | | 19b. TELEPHONE NUMBER *(include area code)* |

## Table of Contents

## INTRODUCTION

TNBC patients have a high incidence of early relapse and metastasis; currently, chemotherapy and targeted therapies (*e.g.* PI3K-AKT inhibition) are the main treatment modalities for TNBC, but one-third of patients develop recurrence and drug resistance within 3 years of therapy. Despite the critical need, the molecular basis for recurrence and drug resistance remains poorly understood. Recently, we have discovered that *LINK-A*, a breast cancer-upregulated lncRNA, interacts with $PIP_3$. *In vitro* and *in vivo* experiments demonstrated that *LINK-A* is critical for breast cancer cell invasiveness and metastasis via its functional role in regulating the PI3K-AKT signaling pathway. Surprisingly, the pan-cancer analysis of *LINK-A* expression in TCGA reveals strong correlation with TNBC and its potential for metastasis. One important goal of the study is to identify *LINK-A* as a novel prognostic biomarker that can reliably stratify patients with TNBC according to clinical outcomes. With the aim of contributing to "precision medicine", a key priority area highlighted by the Department of Defense, Breast Cancer Research Program overarching challenges, we propose to investigate a novel lncRNA-dependent non-canonical PI3K-AKT pathway underlying the metastatic progression of TNBC by using new technologies including RNAScope®, high-throughput sequencing, *in vivo*-grade locked nucleic acids (LNAs), and orthotopic xenograft models of human breast cancer metastasis. Therefore, combinations of PI3K-AKT pathway inhibitors with an LNA-based lncRNA targeting strategy tested in this application may deliver maximum efficacy in TNBC.


## KEY WORDS

TNBC, Long non-coding RNA, PIP3, AKT, Phosphorylation, Locked Nucleic Acids, LNA, AKT inhibitor, Tumorigenesis


## ACCOMPLISHMENTS

Major goals of the project – *Our central hypothesis is that LINK-A functions to regulate the WPI3K-AKT signaling pathway via its interaction with $PIP_3$ in TNBC cells and that this mechanism may impact the efficacy of PI3K-AKT inhibition*. Following an extended evaluation and approval period regarding our animal protocol and human subjects, the grant was completely set up on September 15, 2017. We have established multiple collaborations nation-wide, collected breast cancer tissues, established stable cell lines based on collaborations and generated a transgenic mouse model with support from the PI's start-up funds. We have also completed our expected experimental goals according to the proposed research schedule. Our accomplishments and experimental findings are described in greater, more comprehensive detail in the following section, with respect to each Major Task/milestone.

### Major Task 1: Characterization of interaction between $PIP_3$, *LINK-A*, and AKT.

*Subtask 1: Characterizing the interactions between $PIP_3$, LINK-A, and AKT*

Major activities and Key results:

To characterize *LINK-A*-$PIP_3$ interaction, we performed a fluorescence resonance energy transfer (FRET) assay using soluble, fluorophore-conjugated BODIPY FL-$PIP_3$ as the donor and Alexa-555-streptavidin-labeled biotinylated *LINK-A* as the acceptor to form a FRET pair (**Figure 1A**). When excited at 475 nm, we observed robust FRET signals as indicated by an increase of acceptor emissions at 570 nm with concomitant decreases in the donor emission centered around

513 nm, signifying physical contact between *LINK-A* and $PIP_3$ in *vitro* (**Figure 1A**). The addition of *LINK-A* to BODIPY FL-$PIP_3$ led to a red shift and was accompanied by a reduction in the emission intensity (**Figure 1B**). This allowed for calculation of the binding affinity of *LINK-A*-$PIP_3$ interaction in solution, which was stronger than or similar to known protein-$PIP_3$ interactions (**Figure 1C**). The lipid-binding lncRNA *RP11-383G10.5* served as a control (**Figure 1C**). Together, our data indicate that lncRNA directly associates with $PIP_3$ *in vitro* with high binding affinity.

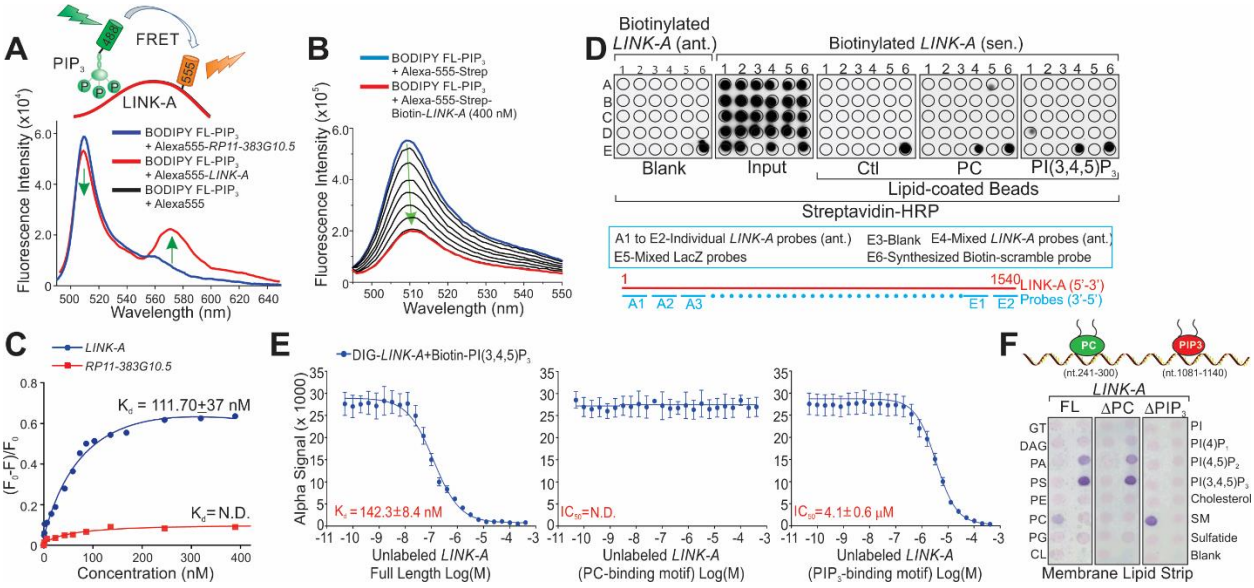


**Figure 1: Characterization of *LINK-A*-$PIP_3$ interaction. A**, Upper panel: graphic illustration of FRET assay. Lower panel: fluorescence spectra of BODIPY FL-PIP3 (donor) in the presence of Alexa-555-Strep (blue) or Alexa-555-Strep-biotin-*LINK-A* (red; λexc=475 nm). **B,** Fluorescence spectra of BODIPY FL-$PIP_3$ upon titration of increasing concentrations of *LINK-A* (0 ~ 400 nM; λexc=490 nm). **C,** $K_d$ value measurement of *LINK-A*-PIP3 interaction. **D,** *In vitro* RNA-lipid binding followed by dot-blot assays (upper panel). Bottom panel: graphic illustration of -oligonucleotides base-pairing *LINK-A* sequence. **E,** Competition binding Alpha assay to determine $K_d$ for interaction between Biotin-$PIP_3$ and DIG-*LINK-A*, in the presence of unlabeled full-length *LINK-A* (left), PC-binding motif (middle) or $PIP_3$-binding motif (right) titrated from 0.4 mM to 0.05 Nm. **F,** Upper panel: graphic illustration of *LINK-A*-PC/$PIP_3$ binding. Lower panel: RNA-lipid overlay assay showing the binding of full-length *LINK-A* and PC- or $PIP_3$-binding region deletion transcripts.

We next mapped the sequences of *LINK-A* that are required for PC and $PIP_3$ binding (**Figure 1D**). Oligonucleotides base pairing with *LINK-A*, *LacZ* sequence, or biotinylated oligonucleotides with scramble sequence were plotted as dot-blot (**Figure 1D**). Pre-incubation of biotinylated *LINK-A* with PC- or $PIP_3$-coated beads protected the lipid-bound *LINK-A* sequences from RNase I digestion, showing streptavidin signals on dots A5 and D1 respectively. Deletion of PC- and $PIP_3$-binding motifs (referred to as ΔPC and Δ$PIP_3$ *LINK-A*) abolished *LINK-A*-PC or *LINK-A*-$PIP_3$ binding respectively (**Figure 1D**).

We next performed an Alpha Assay using unlabeled full-length *LINK-A*, synthesized PC binding motif, or $PIP_3$ binding motif as competitors. 142 nM of full-length, unlabeled *LINK-A* were required to inhibit *LINK-A*-$PIP_3$ interaction by half (**Figure 1E**). While the PC-binding motif failed to exhibit any effect, the presence of the $PIP_3$-binding motif showed partial inhibitory effects on *LINK-A*-$PIP_3$ interaction (**Figure 1F**), indicating the importance of 2-D and 3-D structures of RNA molecules for RNA-lipid binding.

To examine the *LINK-A*-$PIP_3$ interaction *in vivo*, RNA immunoprecipitation (RIP) assay using a $PIP_3$ antibody showed *LINK-A*-$PIP_3$ interaction *in vivo*, which was abolished by PI3K inhibitor LY294002 (**Figure 2A**).We then examined the role of *LINK-A* in AKT-$PIP_3$ interaction

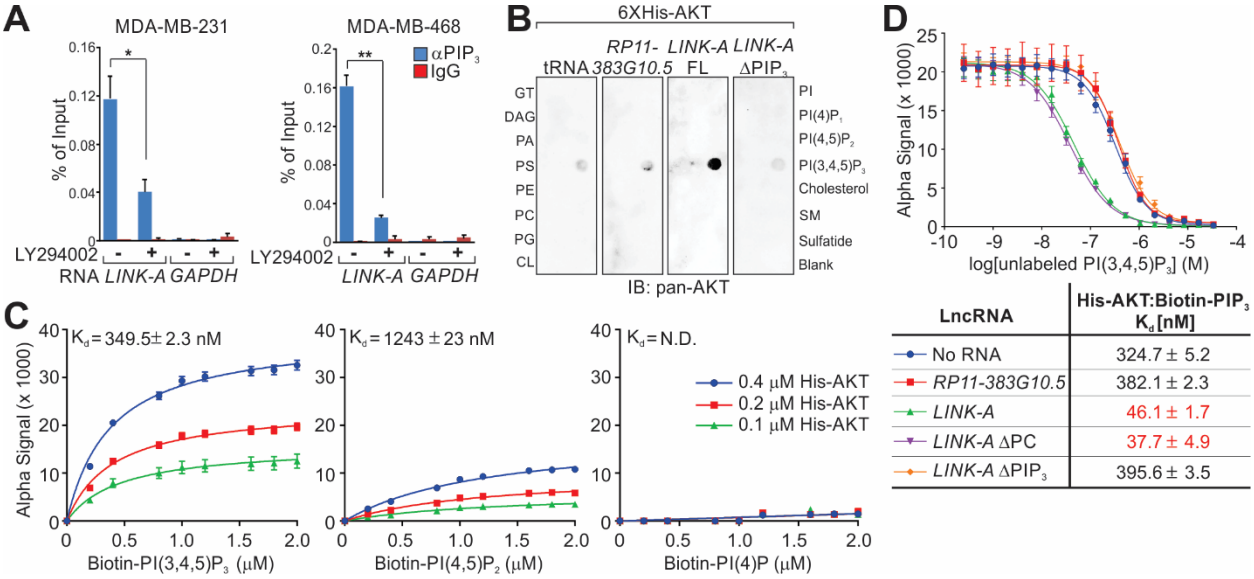


| LncRNA | His-AKT:Biotin-$PIP_3$ $K_d$ [nM] |
|---|---|
| No RNA | 324.7 ± 5.2 |
| *RP11-383G10.5* | 382.1 ± 2.3 |
| *LINK-A* | 46.1 ± 1.7 |
| *LINK-A* ΔPC | 37.7 ± 4.9 |
| *LINK-A* $\Delta PIP_3$ | 395.6 ± 3.5 |

**Figure 2: *LINK-A*-$PIP_3$ interaction promotes recruitment of AKT. A**, RIP-qPCR detection of indicated RNAs retrieved by PIP3-specific antibody in MDA-MB-231 cells treated with DMSO or LY294002. **B,** Lipid-RNA-protein overlay assay revealing AKT-$PIP_3$ interaction in the absence or presence of FL *LINK-A* or $\Delta PIP_3$ deletion transcript. Cardiolipin-binding lncRNA *RP11-383G10.5* serves as a negative control. **C,** Competition binding Alpha assay to determine Kd for interaction between Biotin-$PIP_3$ and DIG-*LINK-A*, in the presence of unlabeled full-length *LINK-A* (left), PC-binding motif (middle) or PIP3-binding motif (right) titrated from 0.4 mM to 0.05 nM. **D,** Top panel: competition binding assay to determine Kd for a biotinylated PIP3 (0.4 μM)-$His_6$-AKT (0.4 μM) interaction in the presence of indicated RNA transcripts. Unlabeled $PIP_3$ was titrated from 33 μM to 0.25 nM. Bottom panel: summary of $K_d$ values region deletion transcripts.

using lipid strips, finding that although recombinant AKT associated with $PIP_3$ *in vitro*, the presence of FL *LINK-A* enhanced the AKT-$PIP_3$ interaction in a $PIP_3$ binding-dependent manner (**Figure 2B**). We further measured the $K_d$ of the AKT-$PIP_3$ interaction in the presence or absence of *LINK-A*. Using Alpha-based saturation and competition assays, we calculated that $K_d$ for the AKT-$PIP_3$ interaction without *LINK-A* is between 304-349 nM, which is consistent with literature (**Figure 2C**). AKT exhibited minor binding with $PIP_2$ ($K_d$=1,243 nM) and no binding with PI(4)P ($K_d$=N.D.) (**Figure 2C**). In the presence of FL but not $\Delta PIP_3$ *LINK-A*, AKT-$PIP_3$ binding was enhanced 16 fold ($K_d$ =19 nM) (**Figure 2D**). These data suggest that AKT, $PIP_3$, and *LINK-A* form a complex upon ligand stimulation, which was confirmed by RIP assay.

Conclusions: Our findings demonstrate that *LINK-A* is the direct interacting partner for $PIP_3$-AKT complex and the presence of *LINK-A* facilitates the recruitment of AKT to $PIP_3$. Using lipid and lncRNA specific techniques, we identified the RNA motif of *LINK-A* which is required for the *LINK-A*-$PIP_3$ interaction. We further determined that the PH domain of AKT is required for the *LINK-A* binding. Hence, our extensive biochemistry studies defined the first lncRNA that associates with phosphor-lipid, $PIP_3$ and AKT.

*Subtask 2: Performing functional rescue experiments to demonstrate that LINK-A-$PIP_3$ interaction is required for AKT activation and downstream cellular activities*

Major activities and Key results:

Rescue experiments after *LINK-A* was knocked down by Locked Nucleic Acids (LNA) and followed by reintroduction of LNA-resistant FL *LINK-A* or *LINK-A* deletion mutants (ΔPC and $\Delta PIP_3$ respectively), indicated that depletion of *LINK-A* diminished *LINK-A*-$PIP_3$ interaction (**Figure 3A**), which was rescued by FL or ΔPC *LINK-A* but not $\Delta PIP_3$ *LINK-A* (**Figure 3B**). These results validate that *LINK-A* bind $PIP_3$ in a specific manner. Next, we examined whether *LINK-A* modulates AKT kinase activity, finding that *LINK-A* knockdown impaired AKT kinase activity in EGF-treated cells and overexpression of FL but not $\Delta PIP_3$ *LINK-A* rescued AKT activation (**Figure 3B**). The presence of FL but not $\Delta PIP_3$ *LINK-A* enhanced AKT enzymatic activity in a polyPIPosomes-mediated *in vitro* assay (**Figure 3B**). These data suggest that *LINK-A* enhances AKT-$PIP_3$ interaction to facilitate the AKT enzymatic activation.

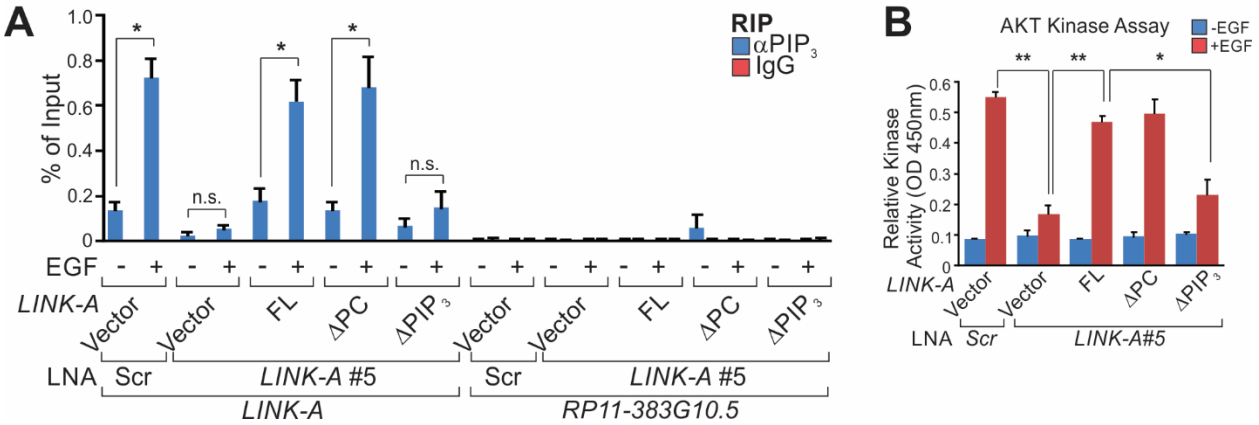


**Figure 3: *LINK-A* promotes enzymatic activation of AKT. A**, RIP-qPCR detection of indicated RNAs retrieved by $PIP_3$-specific antibody in MDA-MB-231 cells harboring indicated LNAs and expression vectors. **B,** Quantification of AKT kinase activity in cell lysates extracted from MDA-MB-231 cells transfected with LNA against *LINK-A* followed by overexpression of indicated vectors and EGF treatment.

Conclusions: We screened and validated that LNAs effectively knockdown *LINK-A* in vivo. Knocking down of *LINK-A* significantly impaired AKT enzymatic activities, which was rescued by *LINK-A* full-length but not the mutants that failed to associate with $PIP_3$. Our results demonstrated that the *LINK-A*-$PIP_3$ interactions are functionally important to mediate the activation of AKT.

*Subtask 3: Examining whether AKT kinase activity is affected by LINK-A* in vitro *and* in vivo

Major activities and Key results:

To examine the *LINK-A*-$PIP_3$ interaction *in vivo*, we took advantage of the MS2-TRAP (MS2-tagged RNA affinity purification) system by expressing MS2 tagged, full-length *LINK-A* or $\Delta PIP_3$ deletion mutant in MDA-MB-231 cells (**Figure 4A**). The GST pull-downed protein-RNA-lipid complex was analyzed by western blot, RT-qPCR, and $PIP_3$ mass ELISA (**Figure 4A-C**). In the presence of the MS2 binding protein (GST-MS2BP), we retrieved similar levels of MS2-*LINK-A* full-length with and without cell permeable $PI(1,4,5,6)P_4$ or $PI(1,3,4,5,6)P_5$ (**Figure 4B**). $PIP_3$ was detected from the protein-RNA-lipid complex in the presence of the vehicle or $PI(1,4,5,6)P_4$ (**Figure 4C**). On the contrary, in the presence of $PI(1,3,4,5,6)P_5$, the

interaction between *LINK-A* and $PIP_3$ was impaired. Further, the MS2 tagged *LINK-A* $\Delta PIP_3$ failed to associate with $PIP_3$ (**Figure 4D-F**).

We determined that there are roughly 150 copies of the *LINK-A per* MDA-MB-231 cell and the copy number was reduced to 10-15 *per* cell by LNA, which was restored by exogenously expressed *LINK-A* or the $\Delta PIP_3$ deletion mutant (**Figure 5A**). *LINK-A* knockdown abolished EGF-induced AKT phosphorylation and cell proliferation (**Figure 5B-C**). Reintroduction of FL *LINK-A*, but not the $\Delta PIP_3$ mutant, restored AKT/GSK-3β phosphorylation and tumor cell proliferation (**Figure 5B-C**). Less than 10 copies of *LINK-A* are found in normal mammary gland epithelial cells (MCF-10A). Stably expressing FL *LINK-A* in MCF-10A cells, to about 150 copies *per* cell, amplified AKT/GSK-3β phosphorylation and cell proliferation (**Figure 5D-F**).

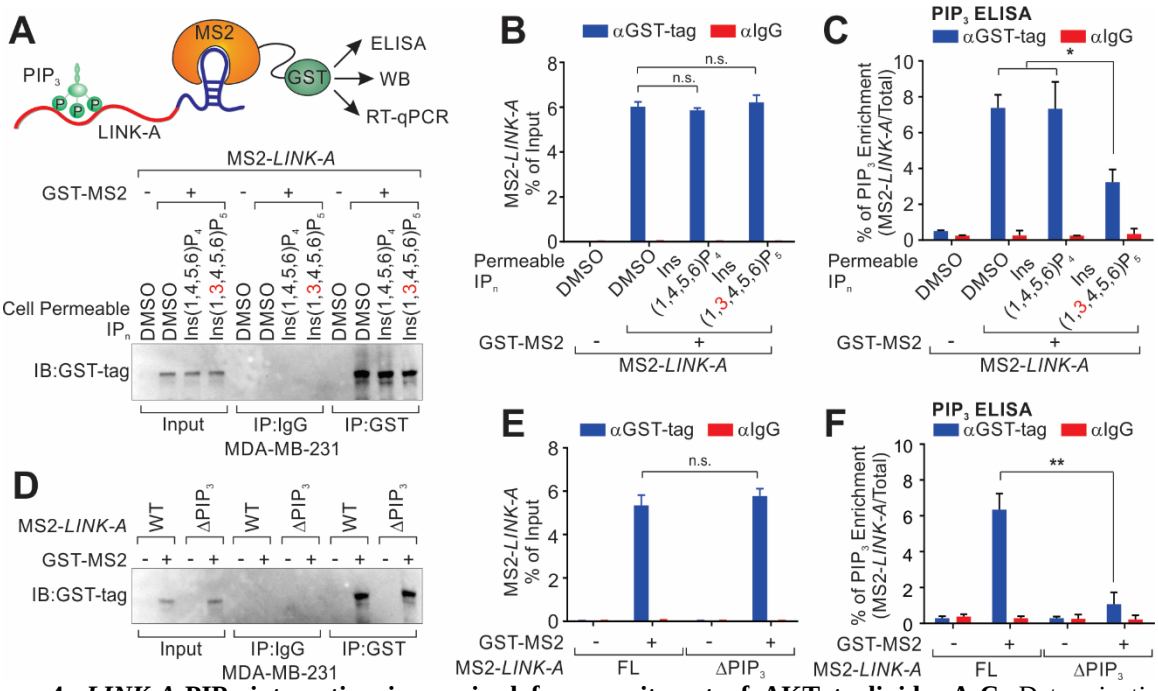


**Figure 4: *LINK-A*-$PIP_3$ interaction is required for recruitment of AKT to lipids. A-C,** Determination of interaction between PIP3 and *LINK-A* by MS2-TRAP assay. Upper panel: schematic illustration of MS2-TRAP assay (A). MS2-tagged *LINK-A* and its associated protein/lipid complexes were pulled down by anti-GST antibodies from cells treated with DMSO, cell permeable $PI(1,4,5,6)P_4$ or $PI(1,3,4,5,6)P_5$ (100 μM, 2 hrs) followed by immunoblotting (A, lower panel), RT-qPCR (B), and PIP3 mass ELISA (C). **D-F,** MS2-TRAP analysis of full-length *LINK-A* or ΔPIP3 deletion mutant associated protein/lipid complexes by immunoblotting (D), RT-qPCR (E), and $PIP_3$ mass ELISA (F).

We used a pair of colorectal cancer cell lines (DLD-1 $PIK3CA^{+/+}$ and DLD-1 $PIK3CA^{+/-}$) in which $PIP_3$ levels were genetically altered. Parental DLD-1 $PIK3CA^{+/+}$ cells harbors about 0.6 pmol $PIP_3$ *per* $5x10^6$ cells before EGF stimulation, and about 2.8 pmol $PIP_3$ after EGF stimulation (**Figure 6A**). In DLD-1 $PIK3CA^{+/-}$ cells, the $PIP_3$ level *per* $5x10^6$ cells was about 0.2 pmol (**Figure 6A**). Consistently, the EGF-induced AKT phosphorylation at Thr308 and Ser473 were abolished in DLD-1 $PIK3CA^{+/-}$ cells (**Figure 6B**). We also measured the copy number of *LINK-A* in DLD-1 $PIK3CA^{+/+}$ and $PIK3CA^{+/-}$ cells, finding that both cell lines harbored about 10 copies of *LINK-A*. We then chose to deliver the *in vitro* transcribed and capped WT *LINK-A* or mutant intracellularly into DLD-1 cells. We attempted to deliver 150 copies of *LINK-A*, and RT-qPCR indicated that single DLD-1 cells contained about 120 copies of *LINK-A* after delivery, of

which WT *LINK-A*, but not $\Delta PIP_3$ mutant, dramatically enhanced the EGF-induced AKT phosphorylation (**Figure 6C**).

Further, in DLD-1 PIK3CA$^{+/-}$ cells, delivery of $PIP_3$ (3 pmol *per* $5x10^6$ cells) increased cellular $PIP_3$ to about 2.2 pmol *per* $5x10^6$ cells. However, restored cellular $PIP_3$ levels marginally mediated EGF-induced AKT phosphorylation (**Figure 6D**). Delivery of *LINK-A* (150 copies *per* cell) alone minimally affected AKT phosphorylation, while combined delivery of $PIP_3$ and *LINK-A* robustly enhanced AKT phosphorylation (**Figure 6E**). To determine if *LINK-A*-$PIP_3$ interaction but not either alone, is important in enhancing the activation of the EGF-AKT pathway, we delivered WT *LINK-A*, $\Delta PIP_3$, or $\Delta PC$ mutants to DLD-1 PIK3CA$^{+/-}$ cells in the presence of $PIP_3$. Despite comparable delivery efficiencies, FL *LINK-* but not $\Delta PIP_3$ mutants enhanced EGF-triggered, $PIP_3$-mediatd AKT phosphorylation (**Figure 6F**). Consistently, co-delivery of $PIP_3$ with WT *LINK-A*, but not 3C, 4A, or 6A mutants in DLD-1 PIK3CA$^{+/-}$ cells led to robust AKT phosphorylation (**Figure 6F**). Furthermore, delivery of ~120 copies of WT *LINK-A*, but not 3C, 4A or 6A mutant, enhanced recruitment of AKT to $PIP_3$ *in vivo* upon EGF stimulation in DLD-1 PIK3CA$^{+/+}$ cells (**Figure 6G**). Taken together, our data indicate that about 150 copies of *LINK-A* is functionally sufficient to facilitate EGF-triggered AKT-$PIP_3$ interaction and subsequent AKT activation.

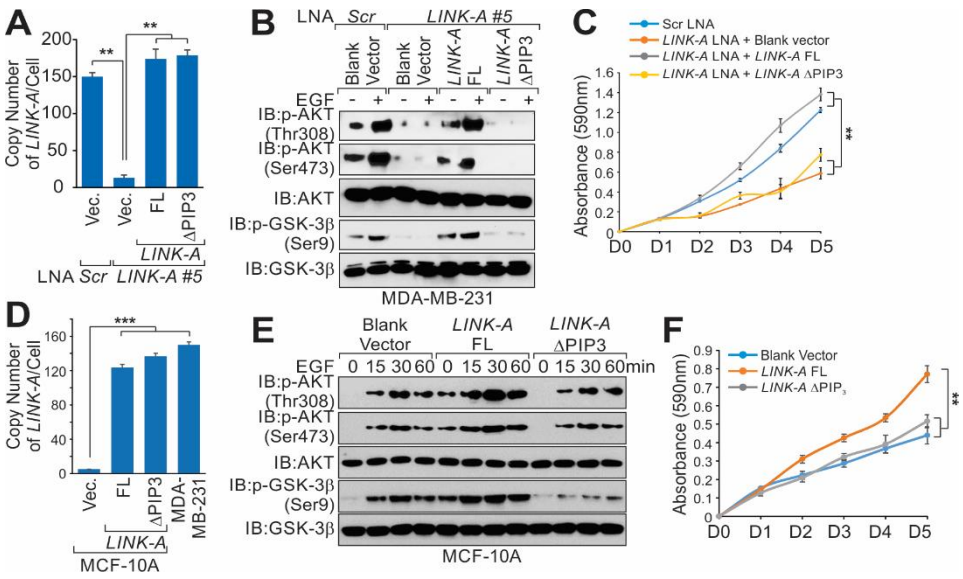


**Figure 5: *LINK-A*-$PIP_3$ interaction promotes AKT activation. A-C,** Determination of *LINK-A* copy number (A), AKT/GSK-3β activation (B) and cell proliferation (C) in MDA-MB-231 cells transfected with LNA against *LINK-A* followed by overexpression of indicated rescue plasmids and EGF stimulation. **D-F,** *LINK-A* copy number (D), AKT/GSK-3β activation (E) and cell proliferation (F) were determined in MCF-10A cells expressing full-length *LINK-A* or $\Delta PIP_3$ deletion mutant, with EGF stimulation.

Conclusions: Taking advantage of MS-TRAP assay and in vivo RNA delivery technologies, we demonstrated that the expression of *LINK-A* with a relative low copy number is sufficient to mediate the phosphorylation and activation of AKT, suggesting that the upregulation of *LINK-A* serves as one of the major molecular mechanisms underlying the resistance to AKT inhibitors of breast cancer patients.

**Major Task 2: Demonstrate the mechanisms of *LINK-A*-dependent AKT Activation**

*Subtask 1: Determining whether the phosphorylation of AKT (Thr308 and Ser473) is regulated by LINK-A upon stimulation with various signals*

Major activities and Key results:

The ErbB receptor tyrosine kinases activate PI3K and downstream AKT in a ligand-dependent manner. We reasoned that *LINK-A*-$PIP_3$ interaction is triggered by epidermal growth factor (EGF) stimulation. We observed that *LINK-A* was enriched in the membrane fraction upon EGF treatment using immuno-RNA Fluorescence in situ hybridization (FISH) (**Figure 7A**). In The presence of EGF stimulation, *LINK-A* faithfully co-localizes with the phosphorylated epidermal growth factor receptor (EGFR) and AKT (**Figure 7A**).

We reasoned that AKT, $PIP_3$, and *LINK-A* form a complex upon ligand stimulation. Further, knockdown of *LINK-A* impaired phosphorylation of AKT at Thr308 and Ser473, under both basal and EGF stimulation conditions, leading to impairment of AKT kinase activity as revealed by diminished phospho-GSK-3β (**Figure 7B**). Next, we examined whether *LINK-A* modulates AKT kinase activity, and we found that expression of *LINK-A* FL but not by $\Delta PIP_3$ *LINK-A* promotes the phosphorylation and activation of AKT in *LINK-A* low expression MCF10A cells (**Figure 7C, D**). It is possible that *LINK-A* may contribute to the stabilization of the AKT-$PIP_3$ interaction, leading to enzymatic activation of AKT *in vitro* and *in vivo*.

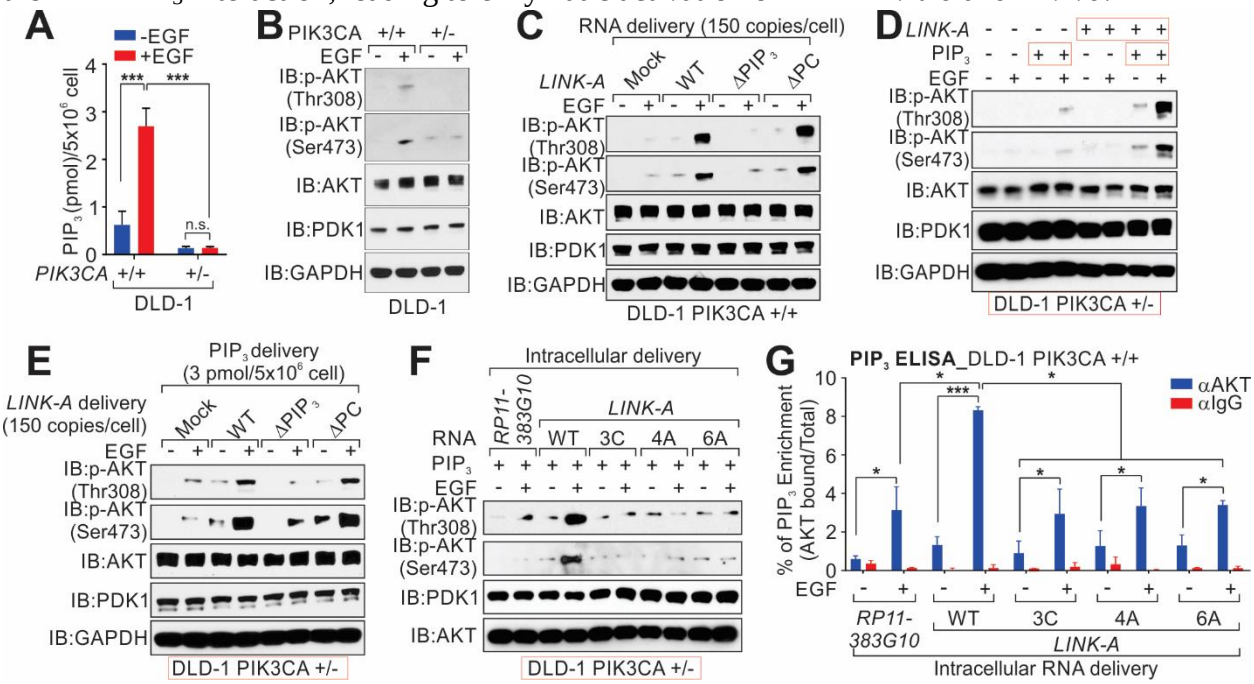


**Figure 6: Functional involvement of *LINK-A*-$PIP_3$ interaction in mediating AKT activation. A-B,** Detection of $PIP_3$ (A) and phospho-AKT (B) level in DLD-1 PIK3CA$^{+/+}$ or PIK3CA$^{-/-}$ cells with or without EGF stimulation. **C,** IB detection of indicated proteins in DLD-1 PIK3CA$^{+/+}$ cells delivered with indicated RNA transcripts with or without EGF stimulation. **D,** IB detection of indicated proteins in DLD-1 PIK3CA$^{+/-}$ cells delivered with PIP3 and/or *LINK-A* transcripts with or without EGF stimulation. **E,** IB detection of indicated proteins (k) in DLD-1 PIK3CA$^{+/-}$ cells delivered with $PIP_3$ and indicated *LINK-A* deletion transcripts with or without EGF stimulation. **F,** IB detection of indicated proteins in DLD-1 PIK3CA$^{+/-}$ cells delivered with PIP3 and indicated *LINK-A* single nucleotide mutated transcripts with or without EGF stimulation. **G,** Quantification of AKT-associated $PIP_3$ in DLD-1 PIK3CA$^{+/+}$ cells delivered with indicated *LINK-A* single nucleotide mutated transcripts with or without EGF stimulation.

Conclusions: Our data determined that EGF serves as the cellular stimuli that trigger the complex formation between *LINK-A*, $PIP_3$ and AKT. EGF plays important roles in tumorgenesis and progression. Our data indicated that *LINK-A* mediates the oncogenic effect of EGF and AKT, serving as a promising therapeutic target for breast cancer patients.

*Subtask 2: Examining the role of LINK-A in regulating the association between AKT and other protein partners*

Major activities and Key results:

In cancer, hyperactivation of PI3K and AKT directs tumor growth and metastasis. $PIP_3$ serves as the second messenger downstream of PI3K to recruit AKT for enzymatic activation. To dissect the signaling pathway mediated by $PIP_3$-bound *LINK-A* in breast tumor, we surveyed the $PIP_3$-binding proteins in mouse normal mammary gland and breast tumor in the presence of *LINK-A* using Liquid chromatography–mass spectrometry (LC-MS) (**Figure 8A**). Without *LINK-A*, $PIP_3$ and AKT associate with a cohort a lipid-interacting proteins which is consistent with the previous findings (**Figure 8A**). Upon expression of *LINK-A*, in addition to lipid-binding proteins, $PIP_3$ and AKT associates with a group of G-protein-coupled receptors (GPCRs), including Cannabinoid receptor 2 (CNR2), Gamma-aminobutyric acid type B receptor subunit 1 (GABR1), Alpha-2A adrenergic receptor (ADA2A), Muscarinic acetylcholine receptor M4 (ACM4) and Mu-type opioid receptor (OPRM) (**Figure 8A**).

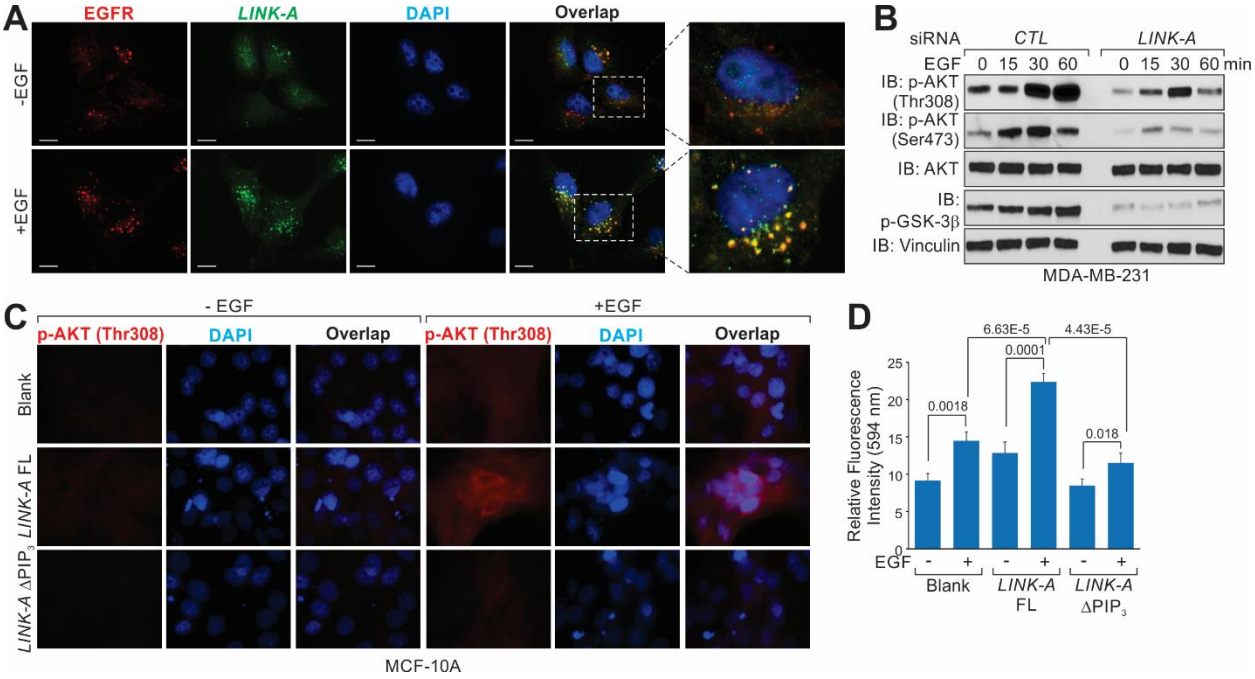


**Figure 7: Expression of *LINK-A* promotes AKT activation. A,** Immunofluorescence labeling using antibodies targeting EGFR and probes targeting *LINK-A* in MDA-MB-231 cells with or without EGF stimulation. Scale bars: 20 μm. **B,** Immunoblotting detection using indicated antibodies of MDA-MB-231 cells harboring indicated siRNAs followed with or without EGF stimulation of indicated time point. **C-D,** Immunofluorescence labeling using antibodies targeting p-AKT (C) or statistical analysis of p-AKT staining intensities (D) in MCF10A cells expressing indicated *LINK-A* expression vectors. Scale bars: 50 μm.

Upon ligand binding, GPCRs activate the associated G protein, by which the G protein alpha subunit can be classified as Gαs, Gαi, Gαq, G12/13. Interestingly, CNR2, GABR1, ADA2A, ACM4 and OPRM all associate with Gαi, leading to inhibition of adenylyl cyclase and reduced cAMP production upon ligand binding[57]. We first determined that $PIP_3$, Gαi, and GPCRs exhibit robust interactions (**Figure 8B**). To address that the $PIP_3$-Gαi-GPCRs interaction is dependent on $PIP_3$ and $PIP_3$-binding *LINK-A*, we performed in vitro GST-pulldown, using *LINK-A* full length (fl) or $PIP_3$-binding motif deletion mutant ($\Delta PIP_3$). Recombinant human GPCRs showed minimal interactions with $PIP_3$, which were marginally detected in the presence

of $PIP_3$. In the presence of $PIP_3$ and *LINK-A* fl, AKT-GPCRs interactions are robustly enhanced. On the contrary, the presence of *LINK-A* $\Delta PIP_3$ mutant failed to do so (**Figure 8B**). The presence of *LINK-A* and $PIP_3$ were confirmed using streptavidin HRP and anti-$PIP_3$ antibody on dot-blots (**Figure 8B**).

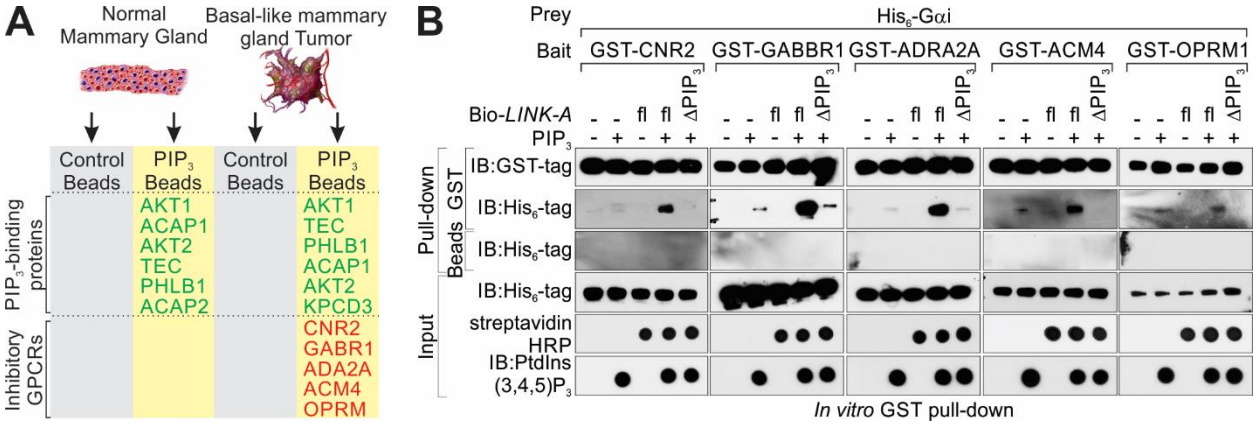


**Figure 8: Identification of GPCRs as $PIP_3$-binding proteins. A,** Mass spectrometry identification of binding protein candidates using $PIP_3$ coated beads or control beads from normal mammary gland to mammary gland tumors. **B,** GST-pulldown followed by immunoblotting detection using indicated recombinant proteins and biotinylated *LINK-A* full-length or $\Delta PIP_3$ mutant.

Conclusions: Our data demonstrated that in normal mammary gland tissues and breast tumor, *LINK-A* facilities the recruitment of AKT to a cohorts of inhibitory GPCRs, leading to the major crosstalk between the $PIP_3$-AKT pathway and GPCR pathways. Our data suggested that in vivo, AKT could be regulated by a cohort of GPCR agonist, such as stress, hypoxia and neuronal transmitters.

*Subtask 3: Identifying the potential novel AKT phosphorylation sites mediated by LINK-A using mass spectrometry*

Major activities and Key results:

Structural analysis has shown that RNA loops may be important for protein associations. The secondary structure of *LINK-A* is involved in its interaction with BRK and LRRK2 and possibly in $PIP_3$ interaction. The 60-nt RNA oligonucleotides of the $PIP_3$ binding motif (nt. 1,081-1,140) harbors an identical stem-loop structure based on computational calculation (**Figure 9A**). We synthesized Digoxigenin (DIG)-labeled 18-nt RNA oligonucleotides harboring wild-type (WT) *LINK-A* sequence (nt.1,100-1,117, 5'-CAGGGUAGACUCGCUCUG-3', loop underlined), RNA oligonucleotides with the 4 central nucleotides of the loop removed or single nucleotides of the loop region mutated (**Figure 9A**).

Alpha assay indicated an adequate interaction between WT *LINK-A* and $PIP_3$ *in vitro*, with $K_d$ of 2.6 μM (**Figure 9B**). Deletion of the loop region (Δ2-5) abolished RNA-$PIP_3$ interaction (**Figure 9B**). Interestingly, RNA oligonucleotides with C to A mutations at either position 4 or 6 showed undetectable interaction with $PIP_3$, suggesting the importance of nucleotides $C^{1109}$ and $C^{1111}$ of *LINK-A* in mediating $PIP_3$ binding (**Figure 9B**). RNA-PIPs overlay assay also exhibited undetectable association of $PIP_3$ with either *LINK-A*$^{C1109A}$ (referred to as 4A) or *LINK-A*$^{C1111A}$ (referred to as 6A) (**Figure 9C**).

Using a similar strategy, the 18-nt RNA oligonucleotide representing *LINK-A* (nt.1100-1117) directly associated with recombinant AKT *in vitro* (**Figure 9D**). Nucleotide $A^{1108}$ at position 3 of the stem-loop was required to mediate *LINK-A*-AKT interaction. *LINK-A* $A^{1108}$ to C mutant (referred to as 3C) exhibited similar binding to $PIP_3$ as WT *LINK-A*, but impaired binding to AKT *in vitro* (**Figure 9D**).

AKT could be phosphorylated at multiple sites. The PH domain plays key roles in regulating the enzymatic activity of AKT. Hence, we determined the potential conformational change and phosphorylation of AKT PH domain. Crystallographic analysis indicated that AKT PH domain harbors three variable loops (referred as L1, L2, and L3) (**Figure 9E**). The phospho-groups of $IP_4$ forms hydrogen bonds with Lys14 and Arg23, which are flanking L1 (**Figure 9E**). We hypothesized that the formation of *LINK-A*-$PIP_3$-AKT complex may cause potential conformational change and phosphorylation of AKT PH domain. We applied Limited Proteolysis (LiP) followed by liquid chromatography–mass spectrometry (LC-MS) analysis (LiP-LC-MS). The loop regions of AKT PH domain were digested by LiP and were not detected

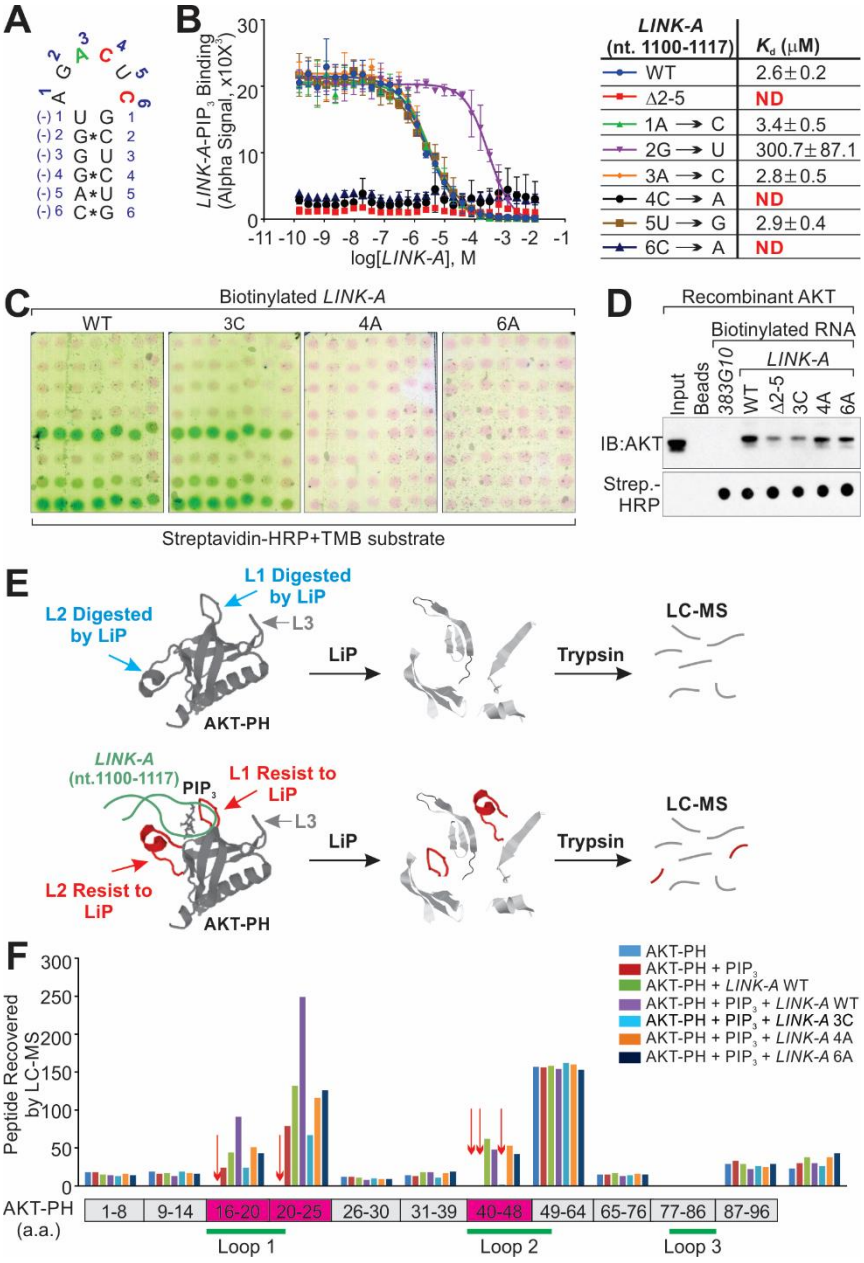


**Figure 9: Molecular mechanisms of *LINK-A*-$PIP_3$-AKT interaction. A,** Schematic illustration of the stem-loop structure of *LINK-A* nt. 1,100-1,117. **B,** Competition Alpha binding assay to determine Kd for a biotinylated $PIP_3$: DIG-*LINK-A* oligonucleotides interaction in the presence of full-length *LINK-A*. **C,** RNA-lipid overlay assay showing the binding of wild-type *LINK-A* or mutants to PIP array using TMB substrates. **D,** In vitro RNA pull-down using biotinylated RNAs as indicated and recombinant AKT. **E,** Schematic illustration of LiP followed by LC-MS. **F**, Recombinant AKT PH domain, and/or $PIP_3$, wild-type *LINK-A*, 3C, 4A or 6A mutant were subjected to LiP followed by LC-MS. Recovered peptide number by LC-MS of AKT PH domain were shown.

by LC-MS (**Figure 9E**). For the $PIP_3$-bound AKT PH domain, L1 resisted partial digestion and was detected by LC-MS, which is consistent with previous studies (**Figure 9F**). Under the same conditions, no peptides were recovered from the L2 region, suggesting that L2 of the AKT PH domain is not involved in interacting with $PIP_3$ (**Figure 9F**). In the presence of *LINK-A*, both L1 and L2 resisted LiP, probably due to *LINK-A*-AKT association and/or potential conformational change of the PH domain (**Figure 9F**). Peptides recovered from the L1 region were increased when both $PIP_3$ and *LINK-A* associated with the PH domain, suggesting a synergistic effect of *LINK-A* in stabilizing the *LINK-A*-$PIP_3$-AKT complex (**Figure 9F**). Furthermore, we indicated that the L2 harbors phosphorylation in the presence of *LINK-A*, suggesting that *LINK-A* medicates post-translational modification of AKT, leading to hyper-activation of AKT. In the presence of *LINK-A* 3C mutant, fewer peptides of L1 and L2 were detected, indicating the reduced synergistic effect when *LINK-A*-AKT interaction was abolished (**Figure 9F**). Furthermore, *LINK-A* 4A and 6A mutants failed to protect L1 from LiP, further supporting the notion that *LINK-A*-$PIP_3$ interaction enhances $PIP_3$-AKT interaction (**Figure 9F**). Two factors that likely contribute to the synergistic effect are: 1) direct *LINK-A*-AKT interaction and 2) AKT conformational change in response to this interaction.

Conclusions: Using open-ended mass spectrometry analysis, we identified the single nucleotides of *LINK-A* that are required for $PIP_3$ and AKT binding respectively and provide structural evidence underlying *LINK-A* facilitated AKT-$PIP_3$ interaction and AKT phosphorylation. These results provide the first insight shed lighting on the molecular mechanism of lncRNAs in modulating the recruitment, phosphorylation and enzymatic activation of AKT.

**What opportunities for training and professional development has the project provided?**

Following the process of establishing and arranging all of the necessary collaborative efforts that are essential for the project, the PI has connected and worked with a diverse group of experts across the nation. The tissues and expertise acquired from these efforts have significantly broadened the tools available for current and future research efforts in the PI's laboratory. Through the abundance of resources and opportunities provided by MD Anderson, Qingsong Hu, a postdoctoral fellow, has been mentored in the research techniques and methods frequently utilized in the lab and has attended various seminars and conferences held by research powerhouses in the area to broaden his research knowledge and expertise.

**How were the results disseminated to communities of interest?**

The PI was awarded the Wilson S. Stone Memorial Award by MD Anderson Cancer Center, celebrating the PI's excellence in conducting research that promotes the biomedical sciences. In accepting this award, the PI presented his research focus on noncoding RNA and cancer to the broader institutional community of students, fellows, nurses, physicians, and scientists. We have also maintained close communications with our four advocates, Furjen Deng, Susan Rafte, Bree Sandlin, and Anne Meyn, as they relay our work to their respective advocacy groups.

**What do you plan to do during the next reporting period to accomplish the goals?**

We have strictly adhered to the statement of work in order to successfully complete all outlined tasks within the stated three year time period, although the timeline will be shifted back by one year. Thus, we plan to accomplish all goals that have been proposed for the second year.

## IMPACT

**What was the impact on the development of the principle disciplines of the project?**

In a continued effort to direct all of the proposed collaborative efforts, the PI has grown his network of partner scientists. Additionally, the PI has established an impressive array of tissues that are used as a comprehensive tool for studying various cancer types. The proposed studies dissect the underlying mechanisms through which lncRNAs promote tumorigenesis *in vivo*, which is a new direction for the PI. This research work serves as preliminary data for the PI's next grant application. As supported by the Breakthrough Award, the PI is being shaped into a leader in the fields of lncRNA and breast cancer research, as recognized by the Wilson S. Stone Memorial Award for research in the biomedical sciences. The PI's goal is to continue to serve as a leader within the breast cancer community; build a breast cancer noncoding RNA research/education program for junior investigators; and proactively guide breast cancer science and its dissemination.

**What was the impact on other disciplines?**

Our research will reveal the fundamental contribution of noncoding RNAs to various disease states, broadening interest in noncoding RNA involvement in various disease processes.

**What was the impact on technology transfer?**

We will provide the *LINK-A* ΔPIP3 stable cell line and pertinent *LINK-A* transgenic animal models to laboratories that are interested in further investigating this topic, after we conclude our research and publish our findings.

**What was the impact on society beyond science and technology?**

Therapeutic options for TNBC patients have been limited due to the interwoven signaling pathways that complicate the development of targeted therapies for TNBC. The proposed study will dissect the molecular mechanisms of lncRNA-dependent resistance to AKT inhibitors, which will highlight their clinical potential as diagnostic indicators, stratification markers, and therapeutic targets. Clinically, the lncRNA-directed targeted therapy using LNAs could serve as a promising strategy to improve outcomes for TNBC patients. This proposal impacts the field of breast cancer research by elucidating genetic evidence for the contribution of lncRNAs as oncogenes that promote breast cancer initiation and progression. Successful completion of this research will contribute to pioneering efforts to develop and mature the field of personalized medicine, specifically with regards to LNAs against TNBC relevant lncRNAs.

## CHANGES/PROBLEMS:

**Actual or anticipated problems or delays and actions or plan to resolve them**

Due to circumstantial delays in the funding process for our research work, we were unable to begin working towards our scheduled/expected tasks and milestones for approximately one year. Consequently, we anticipated our research schedule to be pushed back in accordance with this factor. However, we have adhered to our expected research schedule following initiation of the experimental process and have experienced no delays with the acquisition of data, collaborative efforts, and research expectations associated with each subtask for this 12 month period.

## PRODUCT

**Publication**

1. Lin C., and Yang L., Long Noncoding RNA in Cancer: Wiring Signaling Circuitry. ***Trends in Cell Biology*** 28, 4, p. 287-301 15 p. (2018)

**Honors**

2016 Wilson S. Stone Memorial Award for young research in the biomedical sciences
2018 Wall of Science Award for Outstanding Scientific Research, Institutional Research Executive Committee, MD Anderson
2018 Andrew Sabin Family Foundation Fellows Award, MD Anderson Cancer Center

**Invited Presentations:**

2016 Wilson S. Stone Award presentation "LncRNA Wire Up Cancer Signaling", "Cancer Evolution: Mechanisms of Vulnerability and Resistance", MD Anderson, Houston, TX
2016 Unlocking Phospholipid-binding Long Non-coding RNAs for Breast Cancer Treatment, Chinese Bioscience Investigator Society, Chinese Bioscience Investigator Society, Chengdu, China
2016 Geoffrey Rosenfeld Symposium, "Unlocking Long Non-coding RNAs for Cancer Treatment," University of California San Diego, University of California San Diego, San Diego, CA
2017 Progress, paradigms, and pathways of long non-coding RNAs in cancer, Nanjing Medical University, The 2nd Forum on Signaling Pathways and Non-coding RNAs in Carcinogenesis, Cancer Prevention and Therapy, Washington DC, MD
2017 Progress, paradigms, and pathways of long non-coding RNAs in cancer, San Antonio Breast Cancer Symposium, San Antonio Breast Cancer Symposium, San Antonio, TX,
2018 Progress, paradigms, and pathways of long non-coding RNAs in cancer, Baylor College of Medicine, Houston, TX

**Participants & Other Collaborating Organizations**

**Special Reporting Requirements**

**Appendices**